Chemisorption and Thermal Decomposition of Methylamine on the Ru(001) Surface

Dale F. Johnson, Youqi Wang, John E. Parmeter,† Malina M. Hills,‡ and W. Henry Weinberg*

Contribution from the Department of Chemical Engineering, University of California, Santa Barbara, California 93106. *Received October 21, 1991*

Abstract: The adsorption and decomposition of monomethylamine on Ru(001) have been studied using high-resolution electron energy loss spectroscopy and thermal desorption mass spectrometry. Molecular adsorption of CH_3NH_2 occurs via lone pair donation of the nitrogen atom, and the desorption of reversibly adsorbed methylamine from a saturated first layer is observed over the temperature range 200–340 K. Thermal decomposition of irreversibly adsorbed methylamine ($\Theta_{CH_3NH_2}$ = 0.15 ± 0.01 monolayer) produces H_2, N_2, NH_3, and surface carbon adatoms. Between 280 and 300 K cleavage of a C–H bond produces μ-η^2-H_2CNH_2, and annealing above 300 K initiates competitive C–H and C–N bond cleavage reactions. The majority path (~70%) results in preferential cleavage of C–H bonds between 300 and 330 K to produce a mixture of η^1-(C)-$HCNH_2$ [ν(CN) = 1450 cm^{-1}] and μ-CNH_2 [ν(CN) = 1640 cm^{-1}] plus hydrogen adatoms. The minority path (~30%) gives rise to C–N bond cleavage between 300 and 320 K to yield short-lived CH_2 and NH_2 intermediates which react to form CH, NH, NH_3, and hydrogen adatoms. The ammonia is stabilized by the presence of electron-withdrawing intermediates and desorbs with a peak temperature of 365 K. Annealing between 330 and 360 K induces N–H bond cleavage in the majority path intermediates to form μ_3-η^2-HCNH [ν(CN) = 1450 cm^{-1}]. Cleavage of the final C–H bond between 370 and 380 K produces η^1-(C)-CNH [ν(CN) = 2275 cm^{-1}] and μ-CNH [ν(CN) = 1665 cm^{-1}], and this is followed by cleavage of the remaining N–H bond between 390 and 400 K to yield μ_3-η^2-CN [ν(CN) = 1660 cm^{-1}]. Rupture of the C–N bond over the temperature range 450–575 K forms carbon and nitrogen adatoms, the latter recombining to desorb as N_2 between 800 and 1000 K leaving only carbon on the surface.

I. Introduction

The study of the interaction of monomethylamine, CH_3NH_2, on the close-packed Ru(001) surface has been undertaken for a number of reasons. The selectivity of this surface toward activating CH, NH, and CN bonds can be determined by studying the decomposition of CH_3NH_2 with thermal desorption mass spectrometry and high-resolution electron energy loss spectroscopy. Such an analysis will also allow for the identification of stable reactive intermediates and, hence, provide insight into the mechanistic details of related catalytic reactions. Finally, it is of interest to contrast the interaction and decomposition of this amine to that of ammonia on the Ru(001) surface, as well as to its chemical reactivity on other single-crystalline surfaces.

The commercial importance of amines, amides, and isocyanates illustrates that there is much to be gained by the study and characterization of CN bond-containing molecules on single-crystalline transition-metal surfaces. Heterogeneous catalytic applications found in practice include hydrodenitrification,[1] reductive amination of alcohols,[2,3] reduction of nitriles,[4] and production of HCN.[5,6] Homogeneous catalytic processes of related importance include hydrocyanation[7] and reductive carbonylation[8] reactions; the former being applied in the manufacture of adiponitrile, $NC(CH_2)_4CN$, used to produce Nylon 66, and the latter being a route to produce aromatic isocyanates and possibly diisocyanates for use in the manufacture of polyurethanes. The isolation and identification of intermediates from the decomposition of methylamine on the close-packed Ru(001) surface will assist in clarifying the mechanistic details of these commercial processes. In particular the dehydrogenated surface species characterized here may play crucial roles in the disproportionation reactions observed to occur during the production of long chain, aliphatic amines.[2,3,9] The findings of this study should be of wide interest and use to researchers in commercially applied catalysis.

Previous studies of monomethylamine on Pt(111),[10,11] Rh(111),[11,12] Mo(100),[13] W(100), and carbon- and oxygen-modified W(100),[14] Cr(111) and Cr(100),[15] Ni(111),[15,16] Ni(100),[15,17] and Pt(100)[18] surfaces have been conducted with a variety of surface-sensitive techniques. Dehydrogenation of methylamine occurs on all surfaces between approximately 300 and 500 K, and the desorption of reversibly adsorbed molecular methylamine ceases near 400 K. The reactivity of each surface toward activating C–N bond cleavage varies dramatically, as determined by the gas-phase products other than H_2 formed from CH_3NH_2 decomposition. On Pt(111) methylamine undergoes no CN bond dissociation with only HCN and cyanogen produced, while on Rh(111), Pt(100), and Mo(100), it experiences partial dissociation as evidenced by cyanogen, HCN, N_2, and surface carbon production. On Ni(111), Ni(100), and W(100) surfaces it is completely dissociated, with only N_2 and surface carbon formed.

† Present address: Division 1126, Sandia National Laboratories, Albuquerque, NM 87185.

‡ Present address: Materials and Mechanics Technology Center, The Aerospace Corp., El Segundo, CA 90009.

(1) (a) Ryan, R. C.; Adams, C. T.; Washecheck, D. M. U.S. Patent 4530911, 1985; *Chem. Abstr.* **1985**, *103*, 382. (b) Laine, R. M. *Catal. Rev. Sci. Eng.* **1983**, *25*, 459–474.

(2) Baiker, A.; Caprez, W.; Holstein, W. L. *Ind. Eng. Chem. Prod. Res. Dev.* **1983**, *22*, 217–225.

(3) Baiker, A.; Richarz, W. *Ind. Eng. Chem. Prod. Res. Dev.* **1977**, *16*, 261–266.

(4) Volf, J.; Pasek, J. In *Catalytic Hydrogenation*; Cerveny, L., Ed.; Studies in Surface Science and Catalysis; Elsevier Science: Amsterdam, 1986; Vol. 27, Chapter 4.

(5) Endter, F. *Platinum Met. Rev.* **1962**, *6*, 9–10.

(6) Pirie, J. M. *Platinum Met. Rev.* **1958**, *2*, 7–11.

(7) Collman, J. P.; Hegedus, L. S.; Norton, J. R.; Finke, R. G. *Principles and Applications of Organotransition Metal Chemistry*; University Science: Mill Valley, CA, 1987; pp 568–571.

(8) Reference 7, pp 643–644.

(9) Adams, R. D.; Kim, H.-S.; Wang, S. *J. Am. Chem. Soc.* **1985**, *107*, 6107–6108; and references therein.

(10) Hwang, S. Y.; Seebauer, E. G.; Schmidt, L. D. *Surf. Sci.* **1987**, *188*, 219–234.

(11) Cordonier, G. A.; Schüth, F.; Schmidt, L. D. *Vacuum* **1990**, *41*, 278–281.

(12) Hwang, S. Y.; Kong, A. C. F.; Schmidt, L. D. *J. Phys. Chem.* **1989**, *93*, 8327–8333.

(13) Walker, B. W.; Stair, P. C. *Surf. Sci.* **1981**, *103*, 315–337.

(14) Pearlstine, K. A.; Friend, C. M. *J. Am. Chem. Soc.* **1986**, *108*, 5842–5847.

(15) Baca, A. G.; Schulz, M. A.; Shirley, D. A. *J. Chem. Phys.* **1985**, *83*, 6001–6008.

(16) Chorkendorff, I.; Russell, J. N., Jr.; Yates, J. T., Jr. *J. Chem. Phys.* **1987**, *86*, 4692–4700.

(17) Schoofs, G. R.; Benziger, J. B. *J. Phys. Chem.* **1988**, *92*, 741–750.

(18) Thomas, P. A.; Masel, R. I. *J. Vac. Sci. Technol. A* **1987**, *5*, 1106–1108.

0002-7863/92/1514-4279$03.00/0

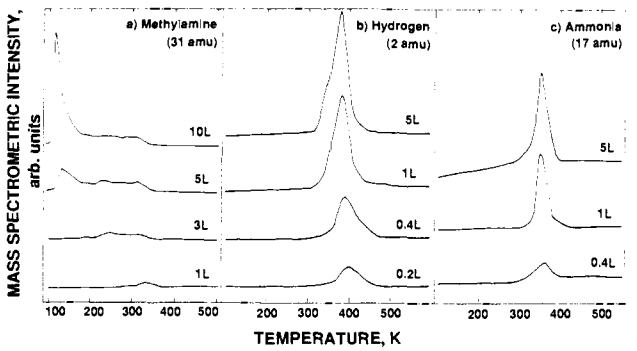

Figure 1. Thermal desorption mass spectra of (a) molecular methylamine, (b) hydrogen, and (c) ammonia following the indicated exposures of CH_3NH_2 on Ru(001) at 80 K and annealed with a heating rate, β, of $\sim$15 K s^{-1}.

II. Experimental Details

The high-resolution EEL spectrometer used in these studies as well as the ultrahigh vacuum chamber in which it is contained have been described in detail elsewhere.[19] Briefly, the stainless steel ultrahigh vacuum (UHV) chamber is pumped by both a 220 L s^{-1} noble ion pump and a titanium sublimation pump which reduce the base pressure to below 10^{-10} Torr. The home-built HREEL spectrometer is of the Kuyatt-Simpson type, with 180° hemispherical deflectors serving as the energy dispersing elements in both the monochromator and the analyzer. The monochromator is spatially fixed, but the analyzer is rotatable to allow off-specular spectra to be measured. On- and off-specular spectra were collected during these experiments, but all spectra presented in this paper were collected in the on-specular direction. The impact energy of the incident electron beam was between 4 and 6 eV in all cases, and the beam was incident on the Ru(001) crystal at an angle of 60° with respect to the surface normal. The instrumental energy resolution in these studies, defined as the full width at half maximum of the elastically scattered beam, varied between 60 and 80 cm^{-1}, while maintaining count rates in the elastic peak between 1.5 and 3.5 $\times$ 10^5 counts s^{-1}.

The Ru(001) crystal was cooled to 80 K with liquid nitrogen and was heated resistively with the temperature monitored by a W–5% Re/W–26% Re thermocouple spotwelded to the back of the crystal. The crystal was cleaned by using periodic ion sputtering and routine annealing to 1000 K in 1 $\times$ 10^{-7} Torr of O_2, followed by annealing to 1625 K in vacuo. Surface cleanliness was determined by both HREELS and H_2 thermal desorption mass spectrometry.

A second UHV chamber was used to conduct the thermal desorption mass spectrometry and low-energy electron diffraction measurements.[20] This chamber also has a base pressure below 10^{-10} Torr using similar pumping techniques. Liquid nitrogen cooling and resistive heating of the Ru(001) crystal were similarly employed. It contains a UTI-100C quadrupole mass spectrometer enclosed in a glass envelope for selective sampling of gases that desorb only from the well-oriented front face of the single crystal. Low-energy electron diffraction optics and a rotatable Faraday cup are available for the display of LEED patterns and the measurement of LEED beam profiles. No ordered LEED structures other than the (1 $\times$ 1) pattern of the unreconstructed substrate were observed following the adsorption of various coverages of methylamine and annealing to higher temperatures. Hence, no LEED results are discussed here. A single-pass cylindrical mirror electron energy analyzer with an integral electron gun is available for Auger electron spectroscopy. The Ru(001) crystal mounted in this chamber was cleaned as described above, and cleanliness was determined by both AES and H_2 thermal desorption mass spectrometry.

Methylamine, CH_3NH_2 (98.0% min)), was obtained from Matheson, and *N,N*-dideuteromethylamine (99.1% minimum, 98% CH_3ND_2) was obtained from MSD Isotopes. Perdeuteromethylamine (98% minimum, 95% CD_3ND_2) was obtained from Protech. All three isotopes of methylamine were further purified by several freeze–pump–thaw cycles prior to use. The purity of all gases was verified by mass spectrometry in both chambers. Gas exposures are reported in units of langmuirs, where 1 langmuir = 1 $\times$ 10^{-6} Torr s. The quoted exposures have not been corrected for the relative ionization probabilities of methylamine and nitrogen.

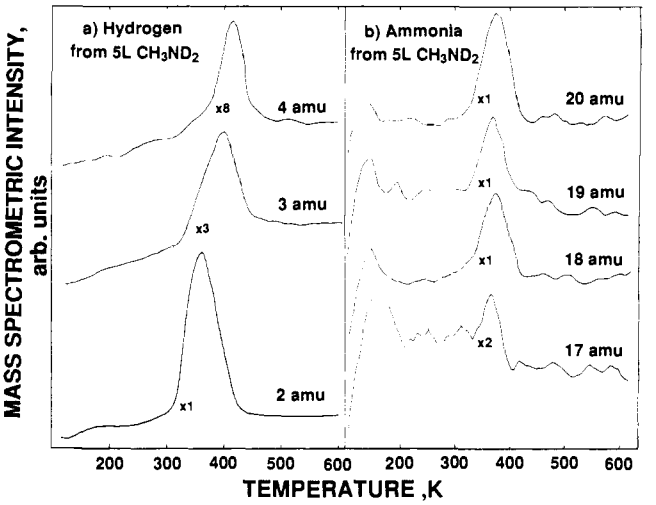

Figure 2. Thermal desorption mass spectra of (a) hydrogen and (b) ammonia following a 5-langmuir exposure of CH_3ND_2 on Ru(001) at 80 K and annealed with a heating rate, β, of $\sim$15 K s^{-1}.

III. Results

A. Thermal Desorption Mass Spectrometry. Thermal desorption spectra measured after the adsorption of CH_3NH_2 and CH_3ND_2 on Ru(001) at temperatures below 100 K and subsequently ramped with heating rates, β, of 15 K s^{-1} are shown in Figures 1 and 2. Only molecular methylamine, hydrogen, nitrogen, and ammonia desorb from these overlayers with surface carbon also deposited as a result of the reaction. In particular, cyanogen, hydrogen cyanide, and methane are not observed. In Figure 1a, molecular methylamine desorbs in a peak at 330 K for low initial coverages of between 0.2 and 1 langmuir, and this peak downshifts and broadens with increasing coverage. Assuming a preexponential factor of the desorption rate coefficient of 10^{13} to 10^{14} s^{-1}, the activation energy of desorption of methylamine at low coverages is estimated by the Redhead method[21] to be 23 $\pm$ 2 kcal mol^{-1}. At intermediate exposures a second peak appears at 240–250 K, which saturates for exposures of 3 to 4 langmuirs. Finally, at high exposures a peak at 130 K, which does not saturate with increasing exposures, appears and is due to desorption from multilayer methylamine.

In addition to reversibly adsorbed CH_3NH_2, the observed desorption of H_2, N_2, and NH_3 indicates that irreversible, dissociative adsorption of methylamine occurs. From Figure 1b, it is seen that with increasing exposures the peak desorption temperature of H_2 shifts from 395 to 375 K. From a saturated monolayer of methylamine, a low-temperature shoulder at approximately 350 K appears. For the heating rate of 15 K s^{-1} employed in these thermal desorption experiments, all of the H_2 is seen to desorb from the surface by 450–460 K.

Ammonia produced from the decomposition of methylamine desorbs over the temperature range of 300 to 400 K with a peak desorption temperature of 365–370 K independent of the initial coverage of methylamine; cf. Figure 1c. This desorption behavior differs from that of similarly low coverages of ammonia on clean Ru(001) where desorption is complete by approximately 360 K and the peak temperature is 315 K.[22,23] Thermal desorption spectra of N_2 (not shown) indicate that the desorption peak temperature shifts from 950 to 875 K with increasing methylamine coverage. This coverage dependence and the high desorption temperatures indicate that desorption results from the second-order recombination of nitrogen adatoms. The desorption of N_2 from the decomposition of ammonia on Ru(001)[24] exhibits a similar coverage dependence although the desorption temperature is

(19) Thomas, G. E.; Weinberg, W. H. *Rev. Sci. Instrum.* **1979**, *50*, 497–501.
(20) Williams, E. D.; Weinberg, W. H. *Surf. Sci.* **1979**, *82*, 93–101.
(21) Redhead, P. A. *Vacuum* **1962**, 203–211.
(22) Benndorf, C.; Madey, T. E. *Surf. Sci.* **1983**, *135*, 164–183.
(23) Parmeter, J. E.; Wang, Y.; Mullins, C. B.; Weinberg, W. H. *J. Chem. Phys.* **1988**, *88*, 5225–5236.
(24) Tsai, W.; Weinberg, W. H. *J. Phys. Chem.* **1987**, *91*, 5302–5307.

approximately 100 K lower. The presence of carbon adatoms causes the recombinative desorption of dinitrogen to occur at higher temperatures by either increasing the ruthenium–nitrogen bond energy, hindering nitrogen adatom surface diffusion via a site blocking mechanism, or a combination of both effects.

Figure 2 shows the thermal desorption spectra of masses 2, 3, and 4 amu (panel a) and masses 17, 18, 19, and 20 amu (panel b) that result from annealing a 5-langmuir exposure of *N,N*-dideuteromethylamine adsorbed at 95 K. The hydrogen isotopes are all desorbed by 460 K with the peak desorption temperatures being 360, 395, and 415 K, respectively, for H_2, HD, and D_2. Thermal desorption of isotopically pure, saturated H and D coverages on clean Ru(001)[25] gives virtually identical desorption spectra with their peak desorption temperatures occurring at 370 K and a high temperature shoulder at 415–420 K.

Figure 2b shows the desorption spectra of ammonia isotopes and their fragments formed from CH_3ND_2. The two parent isotopes, ND_3^+ (20 amu) and ND_2H^+ (19 amu), are responsible for the signals at masses 17 and 18 amu. Cleavage of one N–D bond in ND_3 yields the fragment ND_2^+ as does cleavage of the N–H bond in ND_2H. Likewise, the cleavage of one of the two N–D bonds of ND_2H yields the fragment NDH^+ of mass 17 amu. Mass spectrometric and high-resolution EEL spectroscopic verification of the purity of N,N-dideuteromethylamine eliminates the possibility of H–D exchange at the nitrogen atom in the parent molecule, and hence there is no possibility that these spectrometric fragment signals at 17 and 18 amu arise from ammonia molecules, NH_2D^+ and NH_3^+. Furthermore, as discussed in section IVB, hydrogenation of either surface nitrogen adatoms or deuterated imidogen, ND, to form NH_3 and NH_2D is not at all likely under these ultrahigh vacuum conditions.[24] The integrated areas under the desorption peaks reveal that $ND_3^+ > ND_2^+ > ND_2H^+ > NDH^+$, and that their relative areas, uncorrected for varying spectrometric sensitivities, are respectively 0.42:0.35:0.17:0.06.

The high-resolution EELS data presented in the next section demonstrate that side-on bonded cyano, CN, is formed as the product of complete dehydrogenation of methylamine. The detection of ammonia in the thermal desorption experiments shows that C–N bond cleavage competes with complete dehydrogenation. Analysis of the NH_3 and H_2 thermal desorption spectra resulting from several experiments of saturated coverages of CH_3NH_2 yields the fractional coverages of ammonia and atomic hydrogen: $\Theta_{NH_3} = 0.02 \pm 0.01$ and $\Theta_H = 0.70 \pm 0.03$. These fractional coverages are obtained by comparing the areas of the products to those for saturated exposures of NH_3 and H_2 and applying the known saturated coverages:[22,26] $\Theta_{NH_3}^{satd} = 0.25$ and $\Theta_H^{satd} = 1.00$. Applying a hydrogen mass balance on these data yields a fractional coverage of irreversibly adsorbed methylamine of $\Theta_{CH_3NH_2} = 0.15 \pm 0.01$. Quantification of the branching ratio between competing C–N bond cleavage and complete dehydrogenation reaction paths will be discussed in section IVB.

B. High-Resolution Electron Energy Loss Spectroscopy. While the thermal desorption data suggest the overall course followed by the surface-catalyzed decomposition of methylamine, it is the high-resolution EELS results which allow a *direct* observation of the chemical changes that occur as the reaction proceeds. The production of ammonia indicates that C–N bond breaking takes place in some fraction of the adsorbed CH_3NH_2, and, as will be developed in this section, this path competes with complete dehydrogenation. Careful analysis of the HREEL spectra allows numerous surface intermediates to be identified and, in particular, that one which is present prior to the branching of the reaction and hence common to both competing pathways.

High-resolution EEL spectra were measured with two different types of experimental annealing treatments. In order to coincide with the temperature-dependent features of the thermal desorption spectra, flash annealing ($\beta \approx 20$ K s^{-1}) of the crystal to the desired temperature was followed by rapid cooling to liquid nitrogen temperature. A second series of HREEL spectra to investigate the surface intermediates of the reaction required similarly rapid but careful annealing in order to control the extent of conversion. The spectra in this second set of data were typically measured at 10-degree increments, and upon observing significant change in a spectrum, a second and sometimes third spectrum was obtained at that annealing temperature. Numerous off-specular spectra (typically 5–10°) were measured, and, while none are shown here, the findings of these spectra are embodied in the discussion in the text. During the course of the experiments, CO from the chamber background adsorbed on the crystal. Its surface concentration is always extremely low, and only because of the very large dynamic dipole moment for the CO stretching frequency is it observed in the spectra. Readsorption of methylamine was kept to a minimum by use of a cyropanel throughout the duration of the experiments.

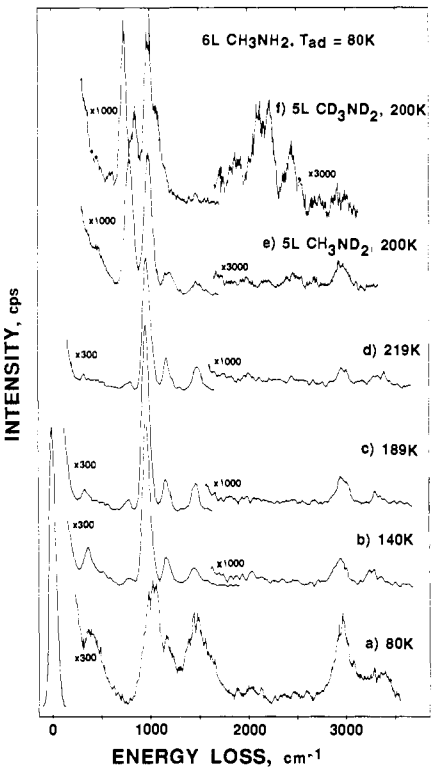

Figure 3. High-resolution EEL spectra resulting from saturation exposures of methylamine and its deuterated isotopes on the Ru(001) surface at 80 K and then annealed rapidly to the indicated temperatures: (a) 80 K, this spectrum is characteristic of partial multilayers of methylamine; (b) 140 K, this spectrum is characteristic of second-layer methylamine; (c) 189 K; (d) 219 K, this spectrum is characteristic of first-layer molecular methylamine; (e and f), 200 K, these spectra are characteristic of first-layer molecular CH_3ND_2 and CD_3ND_2, respectively. See text.

The HREEL spectra following saturation exposures of either CH_3NH_2, CH_3ND_2, or CD_3ND_2 (typically between 4 and 6 langmuir exposures adsorbed at 80–90 K) and subsequently annealed to the indicated temperatures are presented in Figures 3–6. A spectrum characteristic of methylamine multilayers is shown in Figure 3a when the crystal at a temperature of 80 K is exposed to greater than 6 langmuirs of methylamine. Annealing this multilayer coverage to 140 K induces the desorption of the multilayers (cf. Figure 1a) and results in the spectrum of Figure 3b. This spectrum is that of second-layer methylamine, a designation supported by observed changes as the surface is further annealed to above 200 K. The librational mode, or frustrated rotation parallel to the surface plane, R_{xy}, at 365 cm^{-1}, is seen to attenuate upon annealing to 189 K, and its disappearance by 200–220 K coincides precisely with the second-layer desorption results of Figure 1a.

Upon the desorption of the second layer, the overlayer present on the surface is that of a saturated first layer of methylamine. Parts d–f of Figure 3 represent the spectra for molecularly ad-

(25) Feulner, P.; Pfnür, H.; Hofmann, P.; Menzel, D. *Surf. Sci.* **1987**, *184*, L411–L414.
(26) Sun, Y.-K.; Weinberg, W. H. *Surf. Sci.* **1989**, *214*, L246–L252.

Table I. Vibrational Frequencies (cm^{-1}) of First and Second Layer Methylamine and Spectroscopic Reference Data[d]

mode	2nd layer 140 K	satd 1st layer, 200–220 K CH_3NH_2	satd 1st layer, 200–220 K CH_3ND_2	satd 1st layer, 200–220 K CD_3ND_2	CH_3NH_2 gas[a]	CH_3NH_2 solid[b]	CH_3ND_2 gas[a]	CH_3ND_2 solid[b]	CD_3ND_2 gas[a]	CD_3ND_2 solid[b]
$\nu_a(NH_2)$ or $\nu_a(ND_2)$	3240	3255			3427	3331	2556	2484	2556	2485
			2460	2450						
$\nu_s(NH_2)$ or $\nu_s(ND_2)$	3190	3200			3361	3260	2479	2443	2477	2445
$\nu_a(CH_3)$ or $\nu_a(CD_3)$					2985	2942	2985	2941	2238	2220
	2905	2920	2920	2200						
$\nu_a(CH_3)$ or $\nu_a(CD_3)$					2961	2887	2961	2863	2202	2190
$\nu_s(CH_3)$ or $\nu_s(CD_3)$	2840	2865	2895	2085	2820	2793	2817	2801	2073	2061
$\delta(NH_2)$ or $\delta(ND_2)$	1555	1560[c]	1210	n.r.	1623	1651	1234	1220	1227	1217
$\delta_a(CH_3)$ or $\delta_a(CD_3)$					1485	1492	1485	1470	1077	1121
	n.r.	n.r.	n.r.	n.r.						
$\delta_a(CH_3)$ or $\delta_a(CD_3)$					1473	1467	1468	1448	1065	1070
$\delta_s(CH_3)$ or $\delta_s(CD_3)$	1425	1425	1465	1055	1430	1441	1430	1421	1123	1050
$\tau(NH_2)$ or $\tau(ND_2)$	n.o.	n.o.	n.o.	n.o.	1455	1353	1140	1130	1110	1070
$\omega_a(CH_3)$ or $\omega_a(CD_3)$					1195	1172	1187	1189	910	929
	1180	1190	1170	850						
$\omega_s(CH_3)$ or $\omega_s(CD_3)$					1130	1182	1117	1130	880	919
$\nu(CN)$	1000	1025[c]	995	975	1044	1048	997	1005	942	942
$\omega(NH_2)$ or $\omega(ND_2)$	1000	980[c]	780	730	780	955	624	751	601	730
NH_2 or ND_2 torsion	n.o.	n.o.	n.o.	n.o.	264	498	229	360	201	365
$\rho(NH_2)$ or $\rho(ND_2)$	775	780	n.o.	n.o.						
R_{xy}	365									
ν(Ru–N)	n.r.	340	335[c]	n.r.						

[a] Reference 27. [b] Reference 28. [c] Resolved off-specular. [d] Key: n.r., not resolved; n.o. not observed; a, asymmetric; s, symmetric.

sorbed, saturated first-layer coverages of CH_3NH_2, CH_3ND_2, and CD_3ND_2, respectively. Mode assignments for the first- and second-layer methylamine and vibrational gas and solid phase references[27,28] are listed in Table I. It is evident that no bonds have been broken, and, furthermore, the molecule is bonded to the surface through the nitrogen atom's donation of its lone pair of electrons. Evidence for this bonding interaction lies in the strong wagging and overlapping deformation modes of the methyl group, $\omega(CH_3)$ at 1180 cm^{-1} and $\delta_a(CH_3)$ and $\delta_s(CH_3)$ at 1425 cm^{-1}, and the hydrogenic stretching modes, $\nu(NH_2)$ at 3200–3300 cm^{-1} and $\nu(CH_3)$ at 2900–2950 cm^{-1}. The nitrogen's coordination to the surface is borne out by the ν(Ru–N) stretching mode at 340–350 cm^{-1} in the spectra of the three isotopes between 200 and 220 K, in excellent agreement with that observed for NH_3 on Ru(001).[23]

Annealing the saturated first layer above 220 K results in competitive molecular desorption and conversion, via C–H bond cleavage, to form chemisorbed methyleniminium, CH_2NH_2. From examination of the spectra, these two processes appear to act in consort with one another in that as one molecule desorbs, an active site on the surface becomes available to catalyze the cleavage of a CH bond in a neighboring methylamine molecule. This reaction to form H_2CNH_2 occurs most rapidly over the temperature range of 280–300 K, as illustrated in Figure 4a–c where the deformation modes of the methyl group at 1460 cm^{-1} are lost, while a strong loss feature at 555 cm^{-1} appears. The methyleniminium intermediate coordinates to the surface in a side-on bridging manner in which the carbon and nitrogen atoms bond to neighboring Ru atoms on the surface. This μ-η^2-H_2CNH_2 coordination gives rise to the broad intense loss features observed at 555 cm^{-1} for CH_2NH_2, 540 cm^{-1} for CH_2ND_2, and 510 cm^{-1} for CD_2ND_2 and assigned to the symmetric and antisymmetric stretching modes of the Ru–CN complex. The di-σ bonding configuration is further supported by the agreement of the CH_2 scissoring and wagging modes at 1430 and 1195 cm^{-1}, respectively, to those of di-σ bonded ethylene on clean Ru(001) which appear at 1450 and 1145 cm^{-1}.[29] If the CH_2NH_2 intermediate were π-bonded to the surface, this would require sp^2 hybridization for the carbon and nitrogen atoms, resulting in $\delta(CH_2)$ and $\omega(CH_2)$ frequencies closer to values of unperturbed gas-phase ethylene, i.e., 1444 and 949 cm^{-1}, respectively,[30] or of π-bonded ethylene in Zeise's salt, $K[PtCl_3(C_2H_4)]$,[31] in which $\delta(CH_2)$ = 1515 cm^{-1} and $\omega(CH_2)$ = 975 cm^{-1}. Organometallic analogues of the bridging CH_2NH_2 intermediate have been synthesized and crystallographically characterized by Adams et al.[32] The bridging (dimethylamino)iminium ligand, μ-η^2-H_2CNMe_2, in the triosmium compound, $Os_3(CO)_{10}(\mu$-η^2-$H_2CNMe_2)(\mu$-H) has a C–N bond distance of 1.53 Å and internal bond angles that indicate sp^3 hybridization of both the carbon and

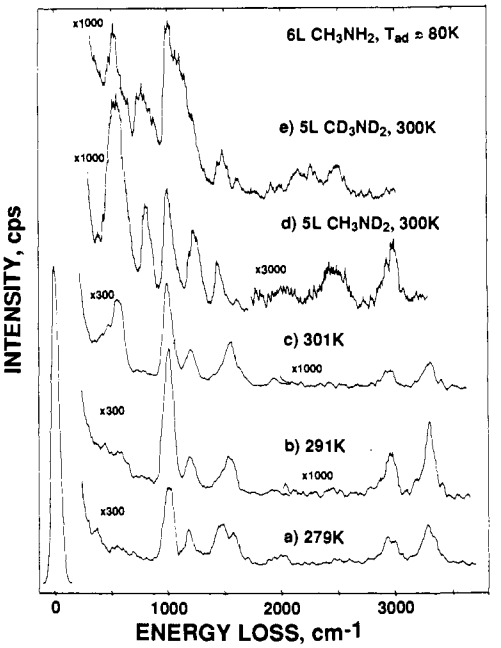

Figure 4. High-resolution EEL spectra resulting from saturation exposures of methylamine and its deuterated isotopes on the Ru(001) surface at 80 K and rapidly annealed to the indicated temperatures: (a and b) 279–291 K, these spectra illustrate the conversion of molecularly adsorbed methylamine to the bridging iminium intermediates; (c) 301 K, this spectrum is characteristic of μ-η^2-H_2CNH_2; (d and e) 300 K, these spectra are characteristic of the deuterated bridging iminium intermediates, μ-η^2-H_2CND_2 and μ-η^2-D_2CND_2, respectively. See text.

(27) Gray, A. P.; Lord, R. C. *J. Chem. Phys.* **1957**, *26*, 690–705.
(28) Durig, J. R.; Bush, S. F.; Baglin, F. G. *J. Chem. Phys.* **1968**, *49*, 2106–2117.
(29) Hills, M. M.; Parmeter, J. E.; Mullins, C. B.; Weinberg, W. H. *J. Am. Chem. Soc.* **1986**, *108*, 3554–3562.
(30) Shimanouchi, T. *Tables of Molecular Vibrational Frequencies*; National Institute of Standards and Technology: Washington, DC, 1972; Consolidated Volume, NSRDS-NBS-39, p 74.
(31) Hiraishi, J. *Spectrochim. Acta, Part A* **1969**, *25A*, 749–760.
(32) (a) Adams, R. D.; Babin, J. E. *Organometallics* **1988**, *7*, 963–969. (b) Adams, R. D.; Babin, J. E.; Kim, H.-S. *Organometallics* **1987**, *6*, 749–754.

Table II. Vibrational Frequencies (cm^{-1}) and Mode Assignments for Side-on Bonded Methyleniminium, μ-η^2-H_2CNH_2, Terminally Bound Secondary Aminocarbene, η^1-(C)-$HCNH_2$, Bridging Aminocarbyne, μ-CNH_2, and Ammonia, NH_3[a,d]

	methyleniminium, 280–320 K			secondary aminocarbene, 310–350 K			aminocarbyne, 310–360 K		ammonia, 310–370 K	
mode	H_2CNH_2	H_2CND_2	D_2CND_2	$HCNH_2$	$HCND_2$	$DCND_2$	CNH_2	CND_2	NH_3	ND_3
$\nu_a(NH_2)$ or $\nu_a(ND_2)$	3340	2510	2510	3250	2450	2450	3250	2450		
$\nu_s(NH_2)$ or $\nu_s(ND_2)$	3300	2400	2450	3175	2325	2325	3175	2325		
$\nu_a(NH_3)$ or $\nu_a(ND_3)$									3250	2500
$\nu_s(NH_3)$ or $\nu_s(ND_3)$										
$\nu_a(CH_2)$ or $\nu_a(CD_2)$	2950	2950	2225							
$\nu_s(CH_2)$ or $\nu_s(CD_2)$	2900	2900	2150							
$\nu(CH)$ or $\nu(CD)$				2920	2920	2200				
$\delta(NH_2)$ or $\delta(ND_2)$	1545	1260	1250	1545	1260	1250	1545	1260		
$\delta(CH_2)$ or $\delta(CD_2)$	1430[b]	1425	1100							
$\delta_s(NH_3)$ or $\delta_s(ND_3)$									1215	1000
$\delta(CH)$ or $\delta(CD)$				740	740	550				
$\pi(CH)$ or $\pi(CD)$				980	980	720				
$\omega(CH_2)$ or $\omega(CD_2)$	1190	1180	900							
$\omega(NH_2)$ or $\omega(ND_2)$	980[b]	810	800	740	550	550	740	550		
$\nu(CN)$	1005	1000	1000	1420	1430	1430	1620	1620		
$\rho(NH_2)$ or $\rho(ND_2)$	790[c]	n.r.	n.r.	1050	750	750	1050	750		
$\rho(CH_2)$ or $\rho(CD_2)$	680[b]	n.r.	n.r.							
$\nu_a(Ru-CN)$	555	540	540							
$\nu_s(Ru-CN)$										
$\nu(Ru-C)$				n.r.	n.r.	n.r.	n.r.	n.r.		
$\nu(Ru-N)$									n.r.	n.r.

[a] Indicated temperatures in the column headings correspond to the ranges in which each intermediate pospulates the surface and influences the high-resolution EEL spectra; refer to text and figures. [b] Resolved off-specular. [c] Reproducibly observed in other HREEL spectra. [d] Key: n.r., not resolved; a, asymmetric; s, symmetric.

nitrogen atoms. The interpretation of the broad intense loss features at 555 cm^{-1} for CH_2NH_2 as the overlapping bridge-bonded symmetric and asymmetric stretching modes is supported by strong infrared absorption bands between 506 and 589 cm^{-1} for bidentate ethylenediamine in Pt, Pd, Cu, and Ni organometallic complexes[33] and also by a very strong HREELS loss feature centered at 565 cm^{-1} for ethylenediamine adsorbed on Pd(111).[34] The complete mode assignments for μ-η^2-H_2CNH_2 and its isotopes present on the surface at 300 K are given in Table II.

Requiring comment beyond the mode assignments of Table II is the appearance of a loss feature at 1430 cm^{-1} in Figure 4e. While this feature is assigned as the symmetric deformation, or scissoring, mode of the CH_2 group in the spectra of H_2CNH_2 and H_2CND_2 in parts c and d of Figure 4, respectively, the intermediate D_2CND_2 generates no loss feature assignable to that observed at 1430 cm^{-1}. The possibility of contamination by some hydrogen-containing methylamine is discarded because the purity of these isotopes was verified by mass spectrometric characterization prior to their use. The appearance of this loss feature results from the reaction having progressed beyond pure D_2CND_2, and there being subsequent decomposition products on the surface as well as the deuterated methyleniminium, D_2CND_2. Additional evidence of the reaction having proceeded beyond pure D_2CND_2 is the comparatively weak ν(Ru–CN) stretching modes at 510 cm^{-1} relative to loss features at 540 and 555 cm^{-1} in the spectra of H_2CND_2 and H_2CNH_2, respectively. While the temperature indicated in Figure 4e is 300 K, it is likely that in the operation of flash annealing the crystal, this temperature was actually overshot slightly, thereby inducing the decomposition reaction to proceed beyond pure CD_2ND_2, vide infra.

Careful annealing of the crystal between 300 and 330 K produces dramatic changes in the spectra as illustrated in Figure 5a–c. Three loss features assignable to bridging methyleniminium at 300 K are no longer present at 330 K: The strong Ru–CN stretching modes at 555–565 cm^{-1}, the CN stretching mode at 1000 cm^{-1}, and the CH_2 stretching modes at 2800–3000 cm^{-1}.

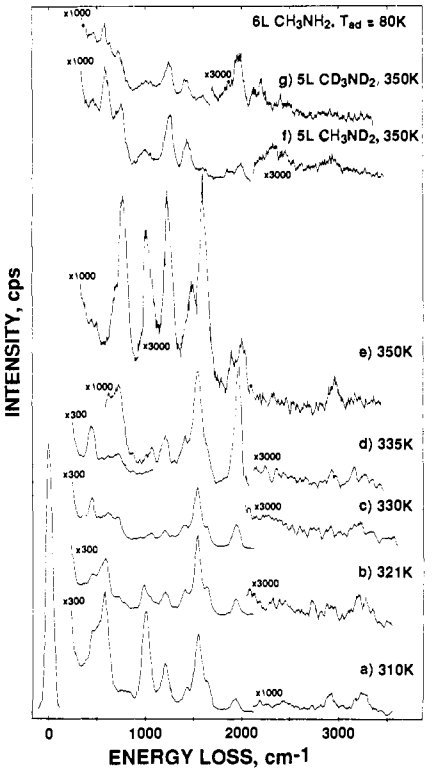

Figure 5. High-resolution EEL spectra resulting from saturation exposures of methylamine and its deuterated isotopes on the Ru(001) surface at 80 K and rapidly annealed to the indicated temperatures: (a and b) 310–321 K, these spectra illustrate the conversion of bridging iminium to the mixture of bridging aminocarbyne and secondary aminocarbene intermediates; (c) 330 K, this spectrum is characteristic of η^1-(C)-$HCNH_2$ and μ-CNH_2; (d and e) 335–350 K, these spectra illustrate the conversion of secondary aminocarbene to formimidoyl; (f and g) 350 K, these spectra are characteristic of mixtures of the deuterated isotopes of the bridging carbyne, secondary aminocarbene, and formimidoyl intermediates. See text.

In place of these loss features appear new peaks at 1070, 1220, and 730 cm^{-1}, accompanied by a noticeable sharpening of the

(33) (a) Adams, D. M. *Metal-Ligand and Related Vibrations*; Edward Arnold: London, 1967; p 309. (b) Powell, D. B.; Sheppard, N. *Spectrochim. Acta* **1961**, *17*, 68–76.

(34) Kordesch, M. E.; Stenzel, W.; Conrad, H. *Surf. Sci.* **1987**, *186*, 601–623.

amine scissoring mode at 1545 cm^{-1} with resolvable features at 1420 and 1640 cm^{-1}. The disappearance of the 1000-cm^{-1} peak assigned to the overlapping ν(CN) and $\omega(NH_2)$ modes of μ-η^2-H_2CNH_2 coincides with the loss of the ν(Ru–CN) stretching modes. The changes seen between 300 and 330 K can be interpreted best by the decomposition of methyleniminium into several new surface products.

Cleavage of one CH bond occurs to form the secondary aminocarbene, $HCNH_2$, which is bound to the surface through the carbon atom only, possibly at an on-top site of a single Ru atom. This terminally bound coordination is represented as η^1-(C)-$HCNH_2$ in which both the carbon and nitrogen atoms are sp^2 hybridized with a partial double bond between them. Back donation from the surface to the antibonding π^* orbital of the planar $HCHN_2$ intermediate serves to yield a CN stretching frequency of 1420–1430 cm^{-1}. The assignment of this loss feature to the ν(CN) of η^1-(C)-$HCNH_2$ is supported by its presence in the spectra of the deuterated isotopes that have been annealed to 350 K in Figure 5f,g.

The precedence for this terminally bound secondary aminocarbene is obtained from organometallic cluster chemistry. Adams et al.[35] in a very thorough series of studies of triosmium cluster compounds have demonstrated the stability of the terminally bound (dimethylamino)carbene ligand, $HCNMe_2$. Its crystallographic characterization yields a CN bond distance of 1.27–1.29 Å, in excellent agreement with that of a CN double bond,[36] and a planar geometry with the carbon and nitrogen both having nearly ideal sp^2 hybridization. Infrared data on the (dimethylamino)carbene ligand are not reported, but as a point of reference the CN stretching frequency in gas-phase methylenimine, $H_2C{=}NH$, is 1638 cm^{-1}.[37]

Cleavage of both CH bonds of the H_2CNH_2 intermediate produces the aminocarbyne intermediate, CNH_2, which has its CN bond axis perpendicular to the surface and bonds in a bridging fashion across a 2-fold surface Ru site. This μ-CNH_2 product is characterized by a very strong scissoring deformation of the NH_2 group and a CN stretching mode of 1640 cm^{-1}. The aminocarbyne intermediate appears to be produced upon annealing the surface above 300 K and is stable to 360 K. (Dimethylamino)carbyne ligands are found in organometallic cluster compounds, such as $Ru_3(CO)_{10}(\mu\text{-}CNMe_2)$ synthesized by Churchill[38] and in a variety of compounds synthesized by Adams et al.[32,35,39]

Both η^1-(C)-$HCNH_2$ and μ-CNH_2 have sp^2 valence hybridization and planar geometries. As a result of this rehybridization, the wagging and rocking modes of the amine group undergo significant shifts. A compilation of documented shifts in these and other modes of $-CH_2$ and $-CH$ groups as the carbon-atom hybridization varies is provided by Ibach and Mills.[40] For both the secondary aminocarbene and the bridging aminocarbyne, the $\omega(NH_2)$ mode has a large red shift to 720–750 cm^{-1}, and the $\rho(NH_2)$ mode has a blue shift to 1070 cm^{-1}. As noted earlier, similar shifts in these fundamental modes of an sp^3-hybridized methylene group are seen for di-σ-bonded ethylene on Ru(001)[29] when compared to sp^2-hybridized methylene groups in gas-phase ethylene and π-coordinated ethylene in Zeise's salt.[30,31]

As will be discussed later in relation to the quantification of the branching ratio between the dehydrogenation and CN bond cleavage reaction pathways, the methyleniminium, H_2CNH_2, is

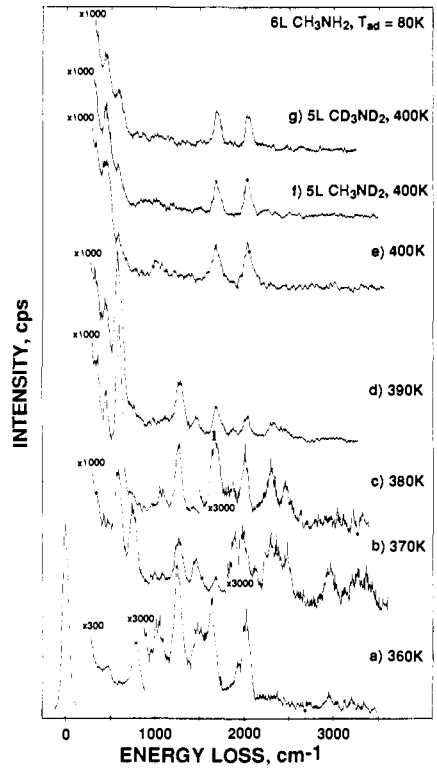

Figure 6. High-resolution EEL spectra resulting from saturation exposures of methylamine and its deuterated isotopes on the Ru(001) surface at 80 K and rapidly annealed to the indicated temperatures: (a) 360 K, this spectrum is characteristic of the mixture of μ-CNH_2 and μ_3-η^2-HCNH, (b and c) 370–380 K, these spectra illustrate the conversion of the overlayer present at 360 K to the mixture of terminally bound and bridge bound hydrogen isocyanide; (d) 390 K, this spectrum is characteristic of η^1-(C)-CNH and μ-CNH; (e–g) 400 K, these spectra are characteristic of μ_3-η^2-CN. See text.

the intermediate from which C–N bond cleavage leads to the production of ammonia. Upon annealing above 300 K and by 330 K the loss feature at 1185 cm^{-1} assigned to the $\omega(CH_2)$ mode of H_2CNH_2 is attenuated and in its place appears a higher energy loss feature at 1215 cm^{-1}. This feature is from the symmetric deformation of the ammonia product, $\delta_s(NH_3)$, and is blue shifted in its frequency due to the presence of electron-withdrawing intermediates on the surface. On clean Ru(001) ammonia's symmetric deformation mode monotonically shifts from 1160 cm^{-1} at low coverages to 1070 cm^{-1} at saturation coverages.[23] In the presence of a p-(1×2) overlayer of oxygen on Ru(001), low coverages of ammonia exhibit $\delta_s(NH_3)$ at 1220 cm^{-1}.[41]

When the C–N bond cleaves, surface methylene and amido groups are formed. Neither CH_2 nor NH_2 are stable surface intermediates on Ru(001) under these conditions: the former dehydrogenating to methylidyne, CH, and hydrogen adatoms, and the latter either dehydrogenating to imidogen, NH, and hydrogen or being hydrogenated to produce adsorbed ammonia.[24,42] High-resolution EELS loss features of methylidyne and imidogen demonstrate CH and NH bending deformation modes at 800 and 1340 cm^{-1}, respectively.[43,44] Methylidyne and imidogen bending modes are unresolved from overlapping loss features of the predominant η^1-(C)-$HCNH_2$ and μ-CNH_2 intermediates. Furthermore, there is such a low coverage of imidogen, methylidyne, and ammonia that their respective loss features are just at or below the HREELS experimental detection limits, and this issue shall

(35) (a) Adams, R. D.; Babin, J. E.; Kim, H.-S.; Tanner, J. T.; Wolfe, T. A. *J. Am. Chem. Soc.* **1990**, *112*, 3426–3435. (b) Adams, R. D.; Babin, J. E.; Kim, H.-S. *J. Am. Chem. Soc.* **1987**, *109*, 1414–1424. (c) Adams, R. D.; Babin, J. E. *Organometallics* **1987**, *6*, 1364–1365. (d) Adams, R. D.; Babin, J. E.; Kim, H.-S. *Inorg. Chem.* **1986**, *25*, 4319–4320. (e) Adams, R. D.; Babin, J. E.; Kim, H.-S. *Organometallics* **1986**, *5*, 1924–1925.

(36) (a) *International Tables for X-ray Crystallography*; Kynoch Press: birmingham, England, 1975; Vol. III, Table 4.2.4, p 276. (b) Pearson, R.; Lovas, F. J. *J. Chem. Phys.* **1977**, *66*, 4149–4156.

(37) Hamada, Y.; Hashiguchi, K.; Tsuboi, M. *J. Mol. Spectrosc.* **1984**, *105*, 70–80.

(38) Churchill, J. R.; DeBoer, B. G.; Rotella, F. J. *Inorg. Chem.* **1976**, *15*, 1843–1853.

(39) Adams, R. D.; Babin, J. E. *Organometallics* **1987**, *6*, 2236–2241.

(40) Ibach, H.; Mills, D. L. *Electron Energy Loss Spectroscopy and Surface Vibrations*; Academic: New York, 1982; pp 193–198.

(41) Wang, Y.; Weinberg, W. H. University of California, Santa Barbara, unpublished results.

(42) George, P. M.; Avery, N. R.; Weinberg, W. H.; Tebbe, F. N. *J. Am. Chem. Soc.* **1983**, *105*, 1393–1394.

(43) Parmeter, J. E.; Hills, M. M.; Weinberg, W. H. *J. Am. Chem. Soc.* **1986**, *108*, 3563–3569.

(44) Parmeter, J. E.; Schwalke, U.; Weinberg, W. H. *J. Am. Chem. Soc.* **1988**, *110*, 53–62.

be dealt with later as the branching ratio is discussed in section IVB. The complete mode assignments for the mixture of η^1-(C)-$HCNH_2$, μ-CNH_2, and NH_3 present on the surface at 330 K (and their deuterated isotopes) are given in Table II.

Over the temperature range 330–360 K, shown in Figures 5c–g and 6a, it is apparent that dehydrogenation at the amine group is occurring. Proof of this statement lies in the significant disappearance of the NH_2 scissoring deformation at 1545 cm^{-1}, which dominates the spectrum of η^1-(C)-$HCNH_2$ at 330 K in Figure 5c. The presence of a loss feature at 1590–1600 cm^{-1} at 350–360 K coupled with the observed frequency shift to 1255 cm^{-1} upon deuteration at the amine group in Figure 5f,g indicates that an intermediate retaining the amine functional group still remains on the surface at 360 K. Coincident with changes in the NH_2 deformation, there appears a very broad and intense loss feature at 720–780 cm^{-1}. This feature was assigned at 330 K to the overlapping δ(CH) and $\omega(NH_2)$ modes of η^1-(C)-$HCNH_2$ and μ-CNH_2, but with the dehydrogenation of most of the amine groups, this very strong feature at 720–780 cm^{-1} is predominantly comprised of a CH bending deformation. A similarly strong CH bending mode is observed at 765 cm^{-1} for molecularly chemisorbed acetylene on Ru(001)[43] in which the carbon atoms are nearly sp^3 hybridized. The loss feature at 1235–1240 cm^{-1} is seen in Figures 5d,e and 6a to maintain its intensity, while that of the $\delta(NH_2)$ signal attenuates and is assignable to an NH deformation mode. The feature at 1440 cm^{-1} does not shift upon either selective or complete deuteration of the intermediate (cf. Figure 5f,g) and is assigned to the CN stretching mode.

The interpretation consistent with these observed changes in the spectra between 330 and 360 K requires separately addressing the fates of the η^1-(C)-$HCNH_2$ and μ-CNH_2 intermediates. Organometallic studies[35b,e,39] have demonstrated that the terminally bound, secondary (dimethylamino)carbene ligand in $Os_3(CO)_9$-$(HCNMe_2)(\mu$-SPh)(μ-H) readily converts to a bridging (dimethylamino)carbyne ligand, μ-$CNMe_2$, upon either pyrolysis at 475 K or photodecarbonylation of the starting compound. Thus, below 360 K the bridging aminocarbyne, μ-CNH_2, is stable, thereby giving rise to the weak, but observed, scissoring deformation of the amine group as well as the CN stretching mode at 1600 cm^{-1}, which is resolved upon deuteration of the methylamine (cf. Figure 5f,g). The marked attenuation of the $\delta(NH_2)$ feature at 360 K relative to 330 K indicates that the population of bridging aminocarbyne is quite low and that the surface at 330 K is populated predominantly by the terminally bound aminocarbene. While the aminocarbyne undergoes no reaction over this temperature range, η^1-(C)-$HCNH_2$ experiences N–H bond cleavage to yield chemisorbed formimidoyl, HCNH, which dominates the surface at 360 K.

On the Ru(001) surface the formimidoyl intermediate has both the carbon and nitrogen atoms bonded to adjacent Ru atoms with the molecular plane tilted across a surface 3-fold site allowing for coordination to a third surface atom either via π electron density donation to the surface or by surface electron density back donation to the adsorbate's π^* antibonding orbital. This triply bridging configuration involving bonding by both the carbon and nitrogen atoms is designated μ_3-η^2-HCNH. The justification for this tilted coordination comes from the CN stretching frequency lying between that for a single and double bond and the appearance of all four bending modes for the CH and NH in Figure 6a. Were the molecular plane of the intermediate parallel to the surface normal, the in-plane deformations, δ(CH) and δ(NH), at 770 and 1235 cm^{-1} would dominate the spectrum and the out-of-plane deformations, π(CH) and π(NH), at 1015 and 1600 cm^{-1} would be detectable only through impact scattering interactions with the incident electron beam, and their vanishing dipolar derivatives in the direction of the surface normal would render their loss features very weak relative to the in-plane deformations. With the formimidoyl intermediate inclined across the 3-fold surface Ru site, both the in-plane and out-of-plane bending modes of the CH and NH groups are indubitably assigned. The final mode assignment consistent with this coordination of HCNH is the CN stretching mode at 1440–1450 cm^{-1}. As noted earlier, the double bond CN stretching frequency is 1638 cm^{-1} in methylenimine,[37] H_2C=NH, and its bond length is 1.273 Å.[36b] With π donation to or π^* back donation from the surface, the CN bond stretching frequency appears at 1440–1450 cm^{-1}, only slightly shifted from the ν(CN) loss feature at 1420–1430 cm^{-1} of the preceding intermediate, η^1-(C)-$HCNH_2$.

A related organometallic analogue to chemisorbed HCNH is the acetimidoyl ligand in the triiron cluster compound, $HFe_3(C$-H_3C=NH)$(CO)_9$.[45] The μ_3-η^2-CH_3C=NH ligand is triply bridging and has a CN bond length of 1.344 Å and a stretching frequency of 1353 cm^{-1}. This virtually planar ligand has the carbon and nitrogen atoms retaining nearly pure sp^2 hybridization, and, while each is coordinated to adjacent Fe atoms, the ligand tilts approximately 45° across the 3-fold site to allow coordination to the third Fe atom. Yin and Deeming[46] also report a triply bridging acetimidoyl ligand in $Os_3(\mu$-H)$(CO)_9(\mu_3$-η^2-CH_3C=NH). On the W(100)-(1×5)-C surface, HCN is purported to undergo self-hydrogenation upon annealing to 475 K to yield terminally coordinated formimidoyl, η^1-(C)-HCNH; HREELS[47] and NEXAFS[48] experiments have been conducted that indicate CN, CH, and NH stretching modes at 1400, 2940, and 3360 cm^{-1}, yet neither CH nor NH deformation modes are reported. The planar HCNH product with sp^2 hybridization at both the carbon and nitrogen is believed to have its CN bond vector inclined at an angle of 58 ± 10° from the surface normal with only the carbon atom bonded to the surface and the molecular plane perpendicular to the surface.

From the preceding analysis it is known that at 350 K the conversion of the secondary aminocarbene, η^1-(C)-$HCNH_2$, to the bridging formimidoyl, μ_3-η^2-HCNH, is not yet complete and that bridging aminocarbyne, μ-CNH_2, is also present. When saturated coverages of CH_3ND_2 and CD_3ND_2 are annealed to 350 K, the spectra of Figure 5f,g are obtained and must be interpreted as mixtures of their respective deuterated aminocarbyne, secondary aminocarbene, and formimidoyl intermediates. Upon deuteration the $\delta(ND_2)$, $\rho(ND_2)$, and $\omega(ND_2)$ appear respectively at 1255, 755, and 580 cm^{-1}, while the δ(ND) and π(ND) modes appear at 1010 and 1255 cm^{-1}. The deformation δ(CD) and π(CD) modes appear at 585 and 715 cm^{-1}, and, of course, the CN bond frequency does not shift noticeably upon deuteration and appears at 1425–1435 cm^{-1}. The complete mode assignments for these chemisorbed species and their deuterated isotopes are provided in Table III.

Annealing between 370 and 390 K induces the changes in the spectra of Figure 6b–d, indicating that both intermediates present at 360 K, μ_3-η^2-HCNH and μ-CNH_2, have undergone dehydrogenation reactions. The very strong δ(CH) mode at 720–780 cm^{-1} is gone from the spectrum at 390 K, and, as it attenuates, a very intense feature at 595–605 cm^{-1} appears. The δ(NH) mode at 1260–1280 cm^{-1} retains its intensity, and by 380 K a resolvable feature at 1665 cm^{-1}, characteristic of a CN double bond, appears. The feature at 1590–1600 cm^{-1}, assigned to the NH_2 scissoring deformation of the low-coverage intermediate, μ-CNH_2, is lost upon annealing to 370 K.

The surface intermediate formed by 380 K and appearing to be stable to 390 K is chemisorbed hydrogen isocyanide, HNC. There are two possible bonding configurations for HNC, and the analogous system of methylisocyanide, CH_3NC, adsorbed on Pt(111) has been thoroughly investigated by Avery and Matheson.[49] Terminal, linear bound CH_3NC revealed a very strong CN stretching frequency of 2240–2265 cm^{-1}, accompanied by a similary strong Pt–C stretch at 385 cm^{-1}. The terminally bound methylisocyanide coexisted at higher coverages with a bridge-

(45) (a) Andrews, M. A.; Kaesz, H. D. *J. Am. Chem. Soc.* **1979**, *101*, 7238–7244. (b) Andrews, M. A.; van Buskirk, G.; Knobler, C. B.; Kaesz, H. D. *J. Am. Chem. Soc.* **1979**, *101*, 7245–7254.
(46) Yin, C. C.; Deeming, A. J. *J. Organomet. Chem.* **1977**, *133*, 123–138.
(47) Serafin, J. G.; Friend, C. M. *J. Phys. Chem.* **1988**, *92*, 6694–6700.
(48) Stevens, P. A.; Madjx, R. J.; Friend, C. M. *Surf. Sci.* **1988**, *205*, 187–206.
(49) (a) Avery, N. R.; Matheson, T. W. *Surf. Sci.* **1984**, *143*, 110–124. (b) Avery, N. R.; Matheson, T. W.; Sexton, B. A. *Appl. Surf. Sci.* **1985**, *22/23*, 384–391.

Table III. Vibrational Frequencies (cm^{-1}) and Mode Assignments of Triply Bridging Formimidoyl, μ_3-η^2-HCNH, Bridging and Terminally Bound Hydrogen Isocyano, μ-CNH and η^1-(C)-CNH, and Triply Bridging Cyano, μ_3-η^2-CN[a]

	formimidoyl, 335–370 K			hydrogen isocyano, 370–390 K[b]		cyano, 400–450 K
mode	HCNH	HCND	DCND	μ-CNH	η^1-CNH	μ^3-η^2-CN
ν(NH) or ν(ND)	3250	2450	2450			
ν(CH) or ν(CD)	2920	2920	2200			
ν(CN)	1450	1450	1450	1660	2280	1670
π(NH) or π(ND)	1450	1220	1220	1450		
δ(NH) or δ(ND)	1240	1000	1000	1280	1060	
π(CH) or π(CD)	950	950	720			
δ(CH) or δ(CD)	770	770	550			
ν_a(Ru–CN)						465
ν_s(Ru–CN)						355
ν(Ru–C)				600	350	

[a] Indicated temperatures in the column headings correspond to the ranges in which each intermediate populates the surface and influences the high-resolution EEL spectra; refer to text and figures. [b] The first overtone of the strong symmetric stretch, ν(Ru–C), combines with the bending deformation, δ(NH), of the bridge-bonded μ-CNH adsorbate to yield a loss feature at 2450 cm^{-1} in Figure 6b–d.

bound imine-like configuration with a characteristic CN double bond stretching frequency that increased with coverage over the range of 1690–1770 cm^{-1}. Very strong Pt–C frustrated translation and skeletal deformation modes were observed at 265 and 530 cm^{-1} for this second bridge-bonded imine-like configuration.

With this information the hydrogen isocyanide intermediate present on the Ru(001) surface at 380–390 K is observed to exist as a mixture of terminally bound, η^1-(C)-CNH, and bridge-bound, μ-CNH. The mode assignments for the two configurations are given in Table III with the CN stretching frequencies at 2275–2295 and 1660–1670 cm^{-1}, respectively, for the terminally bound and bridge bound HNC intermediates. The NH bending deformations are at 1090 cm^{-1} for η^1-(C)-CNH and at 1260–1280 cm^{-1} for μ-CNH. For comparison the NH bending deformation is at 1344 cm^{-1} for gas-phase methylenimine.[37] The very strong loss feature at 595–605 cm^{-1} is assigned to the frustrated translation of the bridge bound hydrogen isocyanide, ν(Ru–C). The appearance of CO on the surface is evidenced by ν(CO) at 2000 cm^{-1}. The amount of CO is quite small, however. The loss feature at 2400–2450 cm^{-1} in Figure 6c,d is puzzling. Its assignment as a combination band of ν(Ru–C) and ν(CO) for the background-adsorbed carbon monoxide is not reasonable since the feature at 2450 cm^{-1} is comparable in intensity to the ν(CO) loss feature itself. The strongest feature is the 595–605 cm^{-1} frustrated translation of the bridging HNC intermediate, and the second strongest loss feature at 1260 cm^{-1} is the bending deformation, δ(NH), of this same intermediate. With both these modes having strong perpendicular dynamic dipole moments for the bridging imine-like configuration, the loss feature at 2400–2450 cm^{-1} is tentatively assigned as the combination of the first overtone of ν(Ru–C) with δ(NH).

Annealing the crystal to 400 K causes dehydrogenation of this remaining NH bond and the conversion to side-on bonded cyano, CN. Parts e–g of Figure 6 correspond to saturation exposures of CH_3NH_2, CH_3ND_2, and CD_3ND_2 adsorbed at 80 K and annealed to 400–425 K. All three isotopes yield identical spectra showing Ru–CN symmetric and asymmetric stretching modes at 340–350 and 585–595 cm^{-1} and ν(CN) stretching modes at 1655–1665 cm^{-1}. The presence of CO present on the surface is noted by the loss features at 450 and 2000 cm^{-1}. Annealing above 425 K desorbs the small amount of CO present on the surface, removing the ν(CO) feature at 2000 cm^{-1} and attenuating that at 450 cm^{-1}. By 450 K thermal decomposition of side-on bonded cyano begins accompanied by an increase in the intensity of the loss feature at 585–595 cm^{-1}. At 600 K no cyano adspecies remains on the surface, as evidenced by the loss of ν(CN), and annealing above 800–900 K initiates recombinative desorption of dinitrogen, decreasing the intensity of the 585–595 cm^{-1} feature but never entirely eliminating it. Thus, the loss feature at 585–595 cm^{-1} present in HREEL spectra above 450 K is due to ν(Ru–C) and ν(Ru–N) of surface carbon and nitrogen adatoms overlapping with the asymmetric ν(Ru–CN) mode of surface cyano present between 400 and 600 K.

Other surface HREELS studies have isolated chemisorbed CN on Pd(111) and Pd(100)[50] and on Cu(111) and O-predosed Cu(111).[51] On both Pd(111) and Pd(100) surfaces, ν(CN) is observed at 220–240 meV (1774–1935 cm^{-1}). On clean Cu(111) ν(CN) is at 2045 cm^{-1}, and on O-predosed Cu(111) it is blue shifted to 2140 cm^{-1}. On Pd(111) and Pd(100) the cyano adspecies is proposed to be side-on bonded with the CN bond vector parallel to the surface. A NEXAFS study[52] of CN/Pd(111) revealed the CN bond axis to be tilted 14° above the plane of the surface, but the authors believe the cyano to be exactly parallel with the 14° tilt resulting from the experimental uncertainty inherent in the measurement. On the Cu(111) surfaces, CN is believed to exist in a side-on bonded configuration on the clean surface, but, when adsorbed onto an O-precovered surface, it reorients to a vertical, terminally bound configuration. This argument is used to explain the observed blue shift and intensification of the loss feature at 2140 cm^{-1} for CN/O–Cu(111) relative to the feature at 2045 cm^{-1} for CN/Cu(111). In our view, this increase in frequency for ν(CN) can more reasonably be explained as resulting from preadsorbed oxygen-withdrawing electron density from the surface and thereby decreasing the extent of back donation to the terminally coordinated CN. On the clean Cu(111) surface the ν(CN) loss feature at 2045 cm^{-1} is too high to be consistent with a side-on bonded configuration but rather reflects a terminally coordinated cyano adspecies bound to the surface predominantly by back donated electron density from the electron-rich, late-transition metallic Cu surface.

As expressed in an earlier publication,[53] the bonding configuration of CN on Ru(001) is best described as μ_3-η^2-CN. Both the carbon and nitrogen atoms interact with the surface: The carbon atom is σ-bonded to a single surface Ru atom while the CN bond vector is inclined across the center of a surface 3-fold site, thereby allowing either the bonding 1π orbitals to donate electron density to the surface or the antibonding 2π orbitals to receive back donated density from the surface. The 4σ lone pair orbital on the nitrogen atom remains collinear with the CN bond vector and thus stays orthogonal to the bonding orbitals between the surface and the cyano adspecies. This μ_3-η^2-CN configuration affords the greatest degree of overlap of surface and adsorbate orbitals and hence is preferred over alternative configurations.

(50) (a) Kordesch, M. E.; Stenzel, W.; Conrad, H. *J. Electron Spectrosc. Relat. Phenom.* **1986**, *39*, 89–96. (b) Kordesch, M. E.; Stenzel, W.; Conrad, H. *Surf. Sci.* **1986**, *175*, L687–L692.

(51) (a) Kordesch, M. E.; Stenzel, W.; Conrad, H.; Weaver, M. *J. Am. Chem. Soc.* **1987**, *109*, 1878–1879. (b) Kordesch, M. E.; Feng, W.; Stenzel, W.; Weaver, M.; Conrad, H. *J. Electron Spectrosc. Relat. Phenom.* **1987**, *44*, 149–162. (c) Feng, W.; Stenzel, W.; Conrad, H.; Kordesch, M. E. *Surf. Sci.* **1989**, *211/212*, 1044–1052.

(52) Somers, J.; Kordesch, M. E.; Linder, Th.; Conrad, H.; Bradshaw, A. M.; Williams, G. P. *Surf. Sci.* **1987**, *188*, L693–L700.

(53) Weinberg, W. H.; Johnson, D. F.; Wang, Y.; Parmeter, J. E.; Hills, M. M. *Surf. Sci. Lett.* **1990**, *235*, L299–L302.

IV. Discussion

The data presented in the previous section allow several important statements to be made regarding the decomposition of methylamine on Ru(001). The demonstrated preference for cleavage of C–H bonds over N–H and C–N bonds is evident from both the thermal desorption and high-resolution EEL spectra, and a comparison of this behavior to that observed for other surface reactions is now possible. Through careful accounting of the ammonia produced from the decomposition of CH_3ND_2, quantification of the branching ratio can be made for the competing dehydrogenation and C–N bond cleavage reaction pathways. Finally, the relevance of this study to commercial disproportionation reactions of aliphatic amines can be discussed.

A. Comparison of CH_3NH_2/Ru(001) to Related Surface Science Studies. The interactions of methylamine on Pt(111), Rh(111), Ni(111), W(100), W(100)–(1×5)–C and W(100)–(1×2)–O, Mo(100), Ni(100), Cr(100), Cr(111), and Pt(100) surfaces have been reported. On Pt(111)[10,11] temperature programmed desorption, TPD, and Auger electron spectroscopy, AES, indicate that no C–N bond cleavage occurs, and dehydrogenation is the only decomposition pathway available to CH_3NH_2. For room temperature exposures only H_2, HCN, and C_2N_2 are observed as decomposition products, and for exposure at 100 K in addition to the above products molecular methylamine also is observed. On Rh(111)[11,12] the decomposition of CH_3NH_2 yields H_2, HCN, and C_2N_2 as it did on Pt(111) except that at ~850 K cyanogen desorption ceases and N_2 desorption is observed. Thus, on Rh(111) there is evidence of C–N bond cleavage seemingly well after methylamine has been completely dehydrogenated to leave surface cyano, CN. High-resolution EELS experiments following the progress of the reaction would certainly help identify the occurrence of any low temperature cleavage of the C–N bond. In contrast, TPD and AES studies of methylamine adsorbed at 87 K on Ni(111)[16] indicate that molecular methylamine, H_2, and N_2 desorb as gas-phase products with surface carbon deposited as all irreversibly adsorbed methylamine experiences complete dissociation of the C–N bond. By approximately 430 K all the H_2 has desorbed, and an Auger line shape analysis indicates that near 410 K carbidic and nitridic species are being formed from C–N bond cleavage of the surface cyano. By study of the H_2 and D_2 thermal desorption spectra from the deuterated isotopes, CD_3NH_2 and CH_3ND_2, it was determined unequivocally that when adsorbed at 412 K, some, if not both, N–H bonds are retained while all the C–H bonds have been cleaved. On W(100) and the carbon and oxygen precovered W(100) surfaces,[14] CH_3NH_2 adsorbed at 120 K undergoes competing molecular desorption and complete decomposition to H_2, N_2, and surface carbon. The carbon precovered surface affected the reaction only by stabilizing the molecular methylamine to higher temperatures, and the oxygen precovered surface oxidized the surface carbon to yield gaseous CO as a product. On Mo(100),[13] thermal decomposition of monomethylamine following room temperature adsorption yields H_2, N_2, HCN, and a small amount of CH_4. No intact molecular CH_3NH_2 is observed, and the HCN product desorbs between 400 and 500 K. High-resolution electron energy loss spectroscopy studies of CH_3NH_2 adsorbed at 300 K on the Ni(111), Ni(100), Cr(111), and Cr(100) surfaces[15] indicate that molecular CH_3NH_2 exists on all surfaces with bonding through the lone pair of electrons on the nitrogen atom. On the Cr surfaces a substantial amount of dissociation is purported to occur based upon the appearance of a very intense, sharp loss feature at 510 cm^{-1} on Cr(100) and an intense, but broad, feature also at 510 cm^{-1} on Cr(111). This loss feature correlates with the surface–adsorbate stretching modes observed here on Ru(001) for the intermediate H_2CNH_2. Temperature programmed reaction spectrometry results of methylamine's decomposition on Ni(100)[17] are remarkably similar to those observed in this study. Molecular methylamine, hydrogen, nitrogen, and ammonia are the observed gaseous products with surface carbon observed with postreaction Auger spectroscopy. The ammonia is seen to have a peak desorption temperature of 365 K, while hydrogen peaks at approximately 375 K. The decomposition of CH_3ND_2 was also examined and showed the ammonia product made up of primarily ND_2H and ND_3, and the H_2 and D_2 desorption spectra had peaks at 370 and 385 K, respectively. On Pt(100)–(5×20) and Pt(100)–(1×1),[18] methylamine's interaction and decomposition were studied. The Pt(100)–(5×20) surface is a stable, pseudohexagonal surface similar to Pt(111), and thermal desorption and high-resolution EELS data indicate that only reversible desorption occurs for methylamine. On metastable Pt(100)–(1×1), however, decomposition is evident from the gas-phase TDS detection of H_2 (T_{pk} ~ 380 K), HCN (550 K), C_2N_2 (780 K), and N_2 (810 K). The appearance of a HREELS loss feature at 1140 cm^{-1} upon annealing to 410 K is assigned to the C–C stretching mode of chemisorbed cyanogen implying completely dehydrogenated cyano, CN, adspecies have dimerized on the surface. Such an assignment must be considered tentative since the HREEL spectrum at 550 K contains evidence of a C–H stretching mode at 2980 cm^{-1}, implying that the 1140-cm^{-1} feature might also arise from a hydrogenic deformation mode of an incompletely dehydrogenated surface intermediate such as HCN.

In addition to the single crystalline studies, the reaction of CH_3NH_2 with H_2 has been examined on other kinds of transition-metal surfaces. Kemball and Moss[54] have studied this reaction over polycrystalline Ni, Fe, Pd, Pt, and W films, while Anderson and Clark[55] examined it over evaporated Pt, Pd, Ni, W, Co, V, and Cu films. The cracking of CH_3NH_2 to CH_4 and NH_3 and disproportionation to di- and trimethylamines were the dominant reaction processes observed. Meitzner et al.[56] studied the reaction over silica-supported Ru, Rh, Re, Pd, Os, Ir, Pt, and Au catalysts and found that cracking to CH_4 and NH_3 occurred on all metals as did a significant amount of disproportionation to dimethylamine, except on Rh. Minor products were found to be produced from the various metals, and most notably Ru and Os converted one-third of the methylamine to acetonitrile. Orita et al.[57] studied the decomposition of CH_3NH_2 at 393 K over Ru black in both the presence and absence of H_2. Of particular relevance is the fact that no higher amines were observed and small amounts of C_2–C_4 hydrocarbons were formed along with the CH_4 and NH_3 cracking products.

A comparison of the interactions of ammonia and methylamine with the Ru(001) surface is of pedagogic interest. The thermal desorption of reversibly adsorbed methylamine, as seen in Figure 1a, contains the same qualitative features as ammonia desorption from clean Ru(001). The desorption temperatures for methylamine are approximately 15 K greater than those of ammonia, and this observation is readily understandable based on the greater Lewis base character of methylamine and noting that both adsorbates bond to the Ru(001) surface via nitrogen lone pair donation. The formation of a second layer of ammonia on Ru(001) gives rise to a resolvable desorption feature at 140 K[22] and a strong librational loss feature at 360 cm^{-1} in HREEL spectra.[23] Methylamine thermal desorption spectra do not reveal a second-layer feature resolved from that of a multilayer of CH_3NH_2. However, the strong librational mode associated with the second layer is readily observed after annealing off the multilayer (cf. Figure 3a–c). Thus, the bonding interactions of ammonia and molecular methylamine are predictably similar with the presence of the methyl group slightly modifying the strengths of the bond to the surface.

B. Branching Ratio: Competing Decomposition Pathways of CH_3NH_2. The majority decomposition pathway available to irreversibly adsorbed methylamine is complete dehydrogenation to chemisorbed cyano, CN. A smaller fraction of methylamine will follow the minority path of carbon–nitrogen bond cleavage, forming the ultimate products of carbon and nitrogen adatoms and ammonia. The production of ammonia occurs subsequent

(54) Kemball, C.; Moss, R. C. *Proc. R. Soc. London, A* **1957**, *238*, 107–116.
(55) Anderson, J. R.; Clark, N. J. *J. Catal.* **1966**, *5*, 250–263.
(56) Meitzner, G.; Myktka, W. J.; Sinfelt, J. H. *J. Catal.* **1986**, *98*, 513–521.
(57) Orita, H.; Naito, S.; Onishi, T.; Tamaru, K. *Bull. Chem. Soc. Jpn.* **1983**, *56*, 3390–3392.

to this C–N bond cleavage step and provides the means for quantifying the branching ratio of the competing decomposition reactions.

The surface reaction that forms ammonia results from amido, NH_2, combining with surface hydrogen. This statement is made based on the observation that for the low coverages of surface hydrogen encountered in this reaction, it is not at all likely that nitrogen adatoms or even imidogen, NH, could be reduced to form ammonia.[24] Thus, the production of ammonia follows the cleavage of the carbon–nitrogen bond in a surface intermediate that has retained the integrity of the amine functional group.

The intermediate which precedes C–N bond cleavage is bridging methyleniminium, μ-η^2-H_2CNH_2, present and stable on the surface at 300 K. The CN bond lengths in two separate triosmium cluster compounds[32] were found to be 1.53 and 1.50 Å, which are elongated relative to the CN single bond length of 1.47 Å.[36a] Heating one of these compounds, $Os_3(CO)_{10}(\mu$-η^2-$H_2CNMe_2)(\mu$-H), to 370 K induces cleavage of a C–H bond to yield a triply-bridging, secondary aminocarbene, μ_3-η^2-$HCNMe_2$, with a C–N bond length of 1.40 Å. The triple-bridging coordination of secondary (dimethylamino)carbene is less favored than its terminally coordinated isomer, η^1-(C)-$HCNMe_2$, which is encountered in numerous other organometallic compounds.[35]

In the decomposition of methylamine on Ru(001), a definitive isolation and identification of μ_3-η^2-$HCNH_2$ has not been made. Mode assignments for such an intermediate would have to include the stretching modes of the Ru–CN framework, which presumably would lie between 500 and 600 cm^{-1}, together with a C–N single bond stretching mode near 1000 cm^{-1} and a C–H deformation mode near 750 cm^{-1}. Such assignments may be possible for the spectra between 310 and 320 K, but the preference of $HCNH_2$ to be sp^2 hybridized and terminally coordinated has been demonstrated, and it is for this reason that triple-bridging secondary aminocarbene is not unambiguously isolated.

The competition between C–H and C–N bond cleavage in methyleniminium begins upon annealing above 300 K and appears to be completed by 320–330 K. The majority pathway continues, after C–H bond cleavage yields $HCNH_2$, and it follows the sequence presented earlier in the interpretation of the HREEL spectra. The minority pathway is initiated by C–N bond cleavage in μ-η^2-H_2CNH_2, leading to the formation of surface methylene, CH_2, and amido, NH_2. As noted previously, both of these intermediates are unstable under these conditions and will quickly convert to further products.

Quantification of the branching ratio is made dependent upon the extent to which the surface amido, NH_2, itself branches to form imidogen and surface hydrogen or is hydrogenated to form ammonia. The key input in addressing this issue lies in the ammonia thermal desorption data and especially that of the mixed deuterated isotopes of ammonia formed from the decomposition of CH_3ND_2 (cf. Figure 2b). The hydrogenation reaction of surface amido involves the transfer of a hydrogen (or deuterium) atom from some surface state (not necessarily a ground state) to the short-lived amido intermediate before the amido itself decomposes. From the thermal desorption spectra of the deuterated ammonia product in Figure 2b, and assuming equal mass spectrometric sensitivities for the parent ND_3 and ND_2H molecules, the amount of ND_2H formed is 40% of that of ND_3, or 28% of the total ammonia, $ND_3 + ND_2H$. Together these two ammonia products account for the observed cracking fragments at masses 17 and 18. The production of ND_3 *must* occur from the deuteration of ND_2, where the deuterium adatom has been formed from the decomposition of a second deuterated amido. This surface deuterium is most likely in a highly mobile surface state where it possesses most of the energy from the decomposition reaction of the unstable ND_2. Upon locating an intact, unstable, but newly formed ND_2, it deuterates this amido and yields the more stable ND_3 product.

The production of ND_2H obviously results from the reaction of ND_2 with the available surface hydrogen adatoms. It is interesting to note that despite the fact that there is significantly higher coverage of surface H than surface D, the fact remains that 72% of the ammonia product is ND_3 while only 28% is ND_2H. This experimental result is simply a manifestation of the difference in relative reaction rates of the deuterated amido, ND_2, with highly mobile D atoms versus thermally equilibrated, less mobile H atoms. The higher reactivity of similarly "hot" hydrogen adatoms has been observed recently in the decomposition of formates on the Ru(001) surface.[58]

The fate of the mobile surface deuterium is not exclusively to react with surface ND_2, but it might also combine with surface hydrogen adatoms and desorb as HD. As seen in Figure 2a, the beginning of HD desorption occurs near 320 K, while that of D_2 is not seen until near 365 K. The preponderance of both the HD and D_2 thermal desorption results from later decomposition of majority path intermediates: η^1-(C)-$HCND_2$, μ-η^2-HCND, μ-CND, and η^1-(C)-CND. The low-temperature tail of the mass 3 amu signal, however, contains H recombination with D released from ND_2 decomposition from the minority path. Thus, a definitive determination of the branching ratio must include the ultimate products of all the surface amido formed when the C–N bonds are cleaved.

For each ND_3 molecule formed, two amido intermediates have to participate, since one of these must decompose in order to release the deuterium atom required to make ND_3. The total ammonia produced from a saturation exposure of CH_3NH_2 was given earlier as 0.02 ± 0.01 monolayer while that of irreversibly adsorbed methylamine was 0.15 ± 0.01 monolayer. With 72% of ammonia formed from CH_3ND_2 being ND_3 and 28% being ND_2H, the most efficient production of ammonia following C–N bond cleavage leads to an estimate of 0.034 monolayer for the fractional coverage of methylamine that follows the minority reaction. In terms of the branching ratio, this result implies that 23%, or one in every four or five, of the irreversibly adsorbed methylamine molecules undergoes C–N bond scission.

As noted above, however, the low temperature tail, 320 K < T < 350 K, of the HD desorption spectrum arises from deuterium and hydrogen recombination, where the deuterium source is the decomposing amido, ND_2. The amount of HD present in the leading edge is estimated to be less than 25% of the total HD produced, and the total fractional coverages of HD and this atomic D in Figure 2a are 0.25 and 0.06 monolayer, respectively, both relative to saturation coverages of atomic deuterium, $\theta_D = 1.00$. The estimate of the maximum amount of amido decomposition that appears as HD is 0.031 monolayer. Combining this with the amount of hydrogenated amido that forms ND_3 yields an estimate of 0.065 for the maximum fractional coverage of methylamine experiencing C–N bond cleavage. In this case the distinction between minority and majority paths is virtually meaningless since 44%, or nearly one of each two molecules, completely dehydrogenates, while the other cleaves its CN bond.

It must be noted, however, that when the C–N bond of methyleniminium is broken, a methylidyne, CH, and hydrogen adatom will be formed upon the decomposition of surface methylene. Methylidyne is stable on Ru(001) to above 500 K and its bending deformation mode, δ(CH), at 800 cm^{-1} is a strong loss feature.[43] The fact that no such HREEL assignment can be made for methylidyne in the spectra from methylamine's decomposition implies that the fractional coverage of methylidyne must be below its detection limit by the HREEL spectrometer. With this in mind, the extent of C–N bond cleavage along the minority pathway is most likely near the lower limits of the above estimates, i.e., between 0.04 and 0.05 monolayer, yielding a branching ratio between one of every three to four irreversibly adsorbed molecules. Scheme I incorporates the principal products of the sequence of elementary reaction steps along the majority and minority paths.

C. η^1-(C)-$HCNH_2$ and the Disproportionation of Amines. Some of the intermediates identified in the decomposition of methylamine on Ru(001) are of general interest because they may play relevant roles in related catalytic processes. For example, the catalytic amination of aliphatic alcohols by copper oxide produces aliphatic amines that are commercially used as corrosion inhibitors and as

(58) Sun, Y.-K.; Weinberg, W. H. *J. Chem. Phys.* **1991**, *94*, 4587–4599.

Scheme I

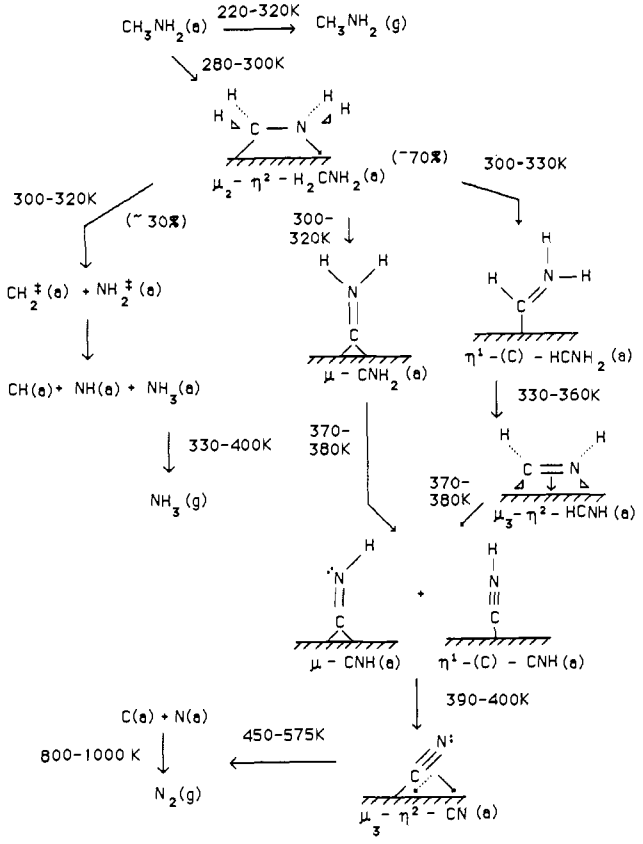

Scheme II

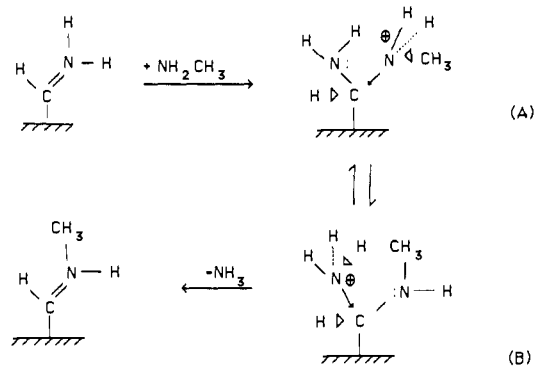

Scheme III

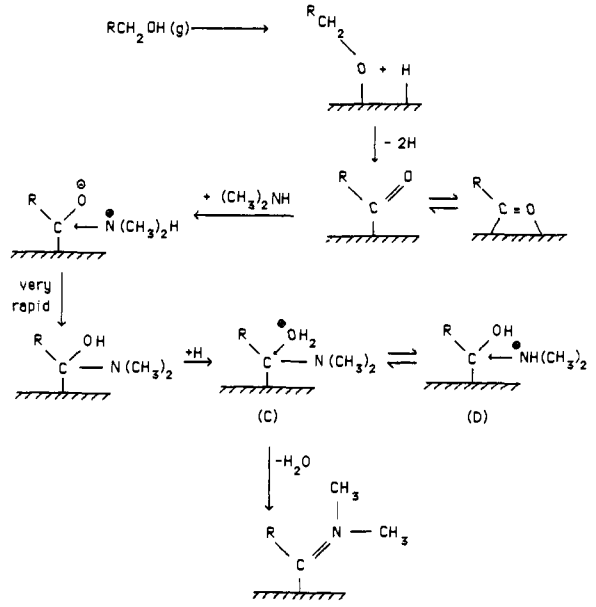

additives to textile products.[3] The process uses either dimethylamine or monomethylamine reacting with long chain primary alcohols to yield the desired amine product and water as in reaction 1. The mechanism has been studied by Baiker et

$$RCH_2OH + (CH_3)_2NH \rightarrow RCH_2N(CH_3)_2 + H_2O \quad (1)$$

al.[2] and it is believed to involve the aldehyde of the reagent alcohol. The selectivity of the reaction is hampered however by disproportionation (reactions 2–4) of the reagent dimethyl- or monomethylamine.[55] At the temperature range of the amination

$$2CH_3NH_2 \rightarrow (CH_3)_2NH + NH_3 \quad (2)$$

$$CH_3NH_2 + (CH_3)_2NH \rightarrow (CH_3)_3N + NH_3 \quad (3)$$

$$2(CH_3)_2NH \rightarrow (CH_3)_3N + CH_3NH_2 \quad (4)$$

process, 400–600 K, the equilibrium mixture consists predominantly of ammonia and trimethylamine. To improve the selectivity of the process, it was discovered that a hydrogen partial pressure of 15–80 kPa in the reaction stream inhibited disproportionation of the feed amine.

In the decomposition of methylamine on Ru(001), the identification of terminally bound, secondary aminocarbene has been made. This planar intermediate has a partial double bond between the carbon and nitrogen, in part due to the incomplete delocalization of the nitrogen lone pair to the empty p_π orbital of the carbon atom. As a result, the carbenoid carbon of η^1-(C)-$HCNH_2$ is electron deficient and susceptible to nucleophilic attack, a chemical property common to metal-coordinated amino carbene ligands.[59] A mechanism for the transalkylation of tertiary amines has been proposed for the (dimethylamino)carbene ligand in $Os_3(CO)_8$ (η^1-$HCNMe_2$)(μ-H)$_2$(μ_3-S) by Adams et al. which involves equilibration between two zwitterionic intermediates.[9] This mechanistic step is illustrated in Scheme II to demonstrate the disproportionation of monomethylamine. The sequence begins with η^1-(C)-$HCNH_2$ experiencing nucleophilic attack at its carbenoid carbon by a second monomethylamine molecule. The cationic pair (A and B) are formed by the intramolecular transfer of a proton between the two amine moieties. The new secondary methylaminocarbene then can be reduced by surface hydrogen to form dimethylamine, $(CH_3)_2NH$.

Related to this reaction mechanism is the amination step of long chain aliphatic alcohols. When α-deuterium labeled alcohols, RCD_2OH, were aminated by dimethylamine, the product mixture contained 33% $RCDHN(CH_3)_2$ and 67% $RCH_2N(CH_3)_2$, but no $RCD_2N(CH_3)_2$.[22] These results indicate that at least one α-CD bond is cleaved during the amination reaction. A mechanism involving an intermediate analogous to η^1-(C)-$HCNH_2$ is proposed in Scheme III to account for the majority product. The aliphatic alcohol will undergo initial O–H bond cleavage on the surface followed by the cleavage of both of the α-CH bonds to yield an intermediate with an electron-deficient carbonyl carbon. This carbon atom is then attacked by the nucleophilic amine, followed by a very rapid intramolecular proton transfer. Protonation from the surface produces the cationic pair (C and D) with water ultimately released as a leaving group upon C–O bond cleavage. The resulting surface intermediate is the secondary (dimethylamino)carbene, which, when reduced by surface hydrogen, yields the desired aliphatic long-chain amine.

V. Summary

A high-resolution electron energy loss spectroscopy and thermal desorption mass spectrometry study of monomethylamine on the clean surface of Ru(001) has been performed, and the important findings are the following:

1. Molecular methylamine coordinates to this surface through lone pair donation of the nitrogen atom, and its interaction is of

(59) (a) Connor, J. A.; Fischer, E. O. *J. Chem. Soc. A* **1969**, 578–584. (b) McCormick, F. B.; Angelici, R. J. *Inorg. Chem.* **1981**, *20*, 1118–1123.

the same nature as that of ammonia with only a slightly stronger bond formed as a result of the substituent methyl group.

2. Preferential dehydrogenation is observed relative to C-N bond cleavage. Approximately ~70% of the irreversibly adsorbed methylamine dehydrogenates completely to surface cyano, μ_3-η^2-CN, with ν(CN) = 1660 cm^{-1}.

3. Activation of C-H bonds is more facile than that of N-H bonds, as judged by the isolation of η^1-(C)-$HCNH_2$ and μ-CNH_2 intermediates.

4. No desorption products other than reversibly adsorbed methylamine are observed to retain the CN bond, and the surface cyano is stable to 450 K at which point it begins to decompose to carbon and nitrogen adatoms.

5. A mechanism for amine disproportionation and amination of aliphatic alcohols is proposed that involves the secondary aminocarbene, η^1-(C)-$HCNH_2$, stable on this surface under these ultrahigh vacuum conditions between 300 and 330 K.

Acknowledgment. This work was supported by the National Science Foundation under Grant No. CHE-90 03553. Additional support was provided by the donors of the Petroleum Research Fund, administered by the American Chemical Society.

Registry No. CH_3NH_2, 74-89-5; Bu, 7440-18-8; H_2CNH_2, 10507-29-6; CH, 3315-37-5; H, 12385-13-6; N_2, 7727-37-9; C, 7440-44-0; $HCNH_2$, 35430-17-2; CNH_2, 84654-89-7; NH_3, 7664-41-7; NH, 13774-92-0.

Long-Lived Oscillations in the Chlorite-Iodide-Malonic Acid Reaction in Batch

Zoltan Noszticzius,*,† Qi Ouyang,† William D. McCormick,† and Harry L. Swinney†

Contribution from the Center for Nonlinear Dynamics and Department of Physics, The University of Texas at Austin, Austin, Texas 78712, and Department of Chemical Physics, Technical University of Budapest, H-1521 Budapest, Hungary. *Received October 28, 1991*

Abstract: The title reaction is the subject of current interest because the first experimental Turing patterns were observed recently in this system. Here we report the first observation of oscillations that are long-lived (over 1 h) in this system in a batch reactor; even after cessation the oscillations can be restarted several times by adding ClO_2 to the exhausted system. These low-frequency low-amplitude (LL) oscillations were detected with both platinum and iodide-selective electrodes in the chlorite-iodide-malonic acid (original CIMA) reaction and in the closely related chlorine dioxide-iodide-malonic acid (minimal CIMA) system. The LL oscillations follow after the already known high-frequency oscillations, sometimes separated by a second induction period. LL oscillations can appear without any induction period if appropriate concentrations of chlorine dioxide, iodomalonic acid, and chloride (CIMA-Cl system) are established in a dilute sulfuric acid medium. In this case neither iodine, iodide, nor malonic acid is needed. Some suggestions are made regarding the mechanism of these newly discovered oscillations.

Introduction

The oscillatory chlorite-iodide-malonic acid (CIMA) system and the closely related chlorine dioxide-iodine-malonic acid oscillator (the "minimal" CIMA system) are presently the focus of much interest.[1-3] The CIMA reaction shows exceptionally rich, dynamical behavior in continuously fed stirred tank reactors[4] and is one of the few simple chemical systems, besides the popular Belousov-Zhabotinsky (BZ) reaction,[5-7] that are capable of producing batch oscillations[8] and traveling chemical waves.[8,9] The principal reason for the renewed interest, however, is the recent discovery, using different types of continuously fed unstirred reactors (CFURs), of the long sought Turing patterns[10,11] in some CIMA systems.[12-15] Experiments in these newly developed, open spatial reactors—the gel ring,[16] the disk,[17] and the membrane[18,19] reactors—exhibited interesting wave behavior[19-21] in the BZ reaction but did not produce stationary Turing structures. A particular reason for the current interest in Turing structures is that they may play a fundamental role in biological pattern formation[11] and morphogenesis. Thus, the first experimental evidence for a Turing bifurcation in a relatively simple chemical system is an important development and focuses interest on the mechanism of the CIMA reaction. Here we report a new type of oscillatory behavior of the CIMA system in batch. These observations suggest some additional features of the mechanism.

The fundamental features of the mechanism were clarified recently by Lengyel, Rábai, and Epstein.[1,2] They discovered that, during the induction period of the CIMA reaction, the chlorite-iodide-malonic acid system was transformed to an oscillatory

* To whom correspondence should be addressed at Technical University of Budapest.
† The University of Texas at Austin.

(1) Lengyel, I.; Rábai, G.; Epstein, I. R. *J. Am. Chem. Soc.* **1990**, *112*, 4606.
(2) Lengyel, I.; Rábai, G.; Epstein, I. R. *J. Am. Chem. Soc.* **1990**, *112*, 9104.
(3) De Kepper, P.; Boissonade, J.; Epstein, I. R. *J. Phys. Chem.* **1990**, *94*, 6525.
(4) Dateo, C. E.; Orban, M.; DeKepper, P.; Epstein, I. R. *J. Am. Chem. Soc.* **1982**, *104*, 504.
(5) Zhabotinsky, A. M. In *Oscillations and Traveling Waves in Chemical Systems*; Field, R. J., Burger, M., Eds.; Wiley: New York, 1985; p 1.
(6) Field, R. J. *Ibid.*; p 55.
(7) Tyson, J. J. *Ibid.*; p 108.
(8) De Kepper, P.; Epstein, I. R.; Kustin, K.; Orban, M. *J. Phys. Chem.* **1982**, *86*, 170.
(9) Weitz, D. M.; Epstein, I. R. *J. Phys. Chem.* **1984**, *88*, 5300.
(10) Turing, A. M. *Philos. Trans. R. Soc. London, B* **1952**, *327*, 37.
(11) Murray, J. D. *Mathematical Biology*; Springer: Berlin, 1989; p 375.
(12) Castets, V.; Dulos, E.; Boissonade, J.; De Kepper, P. *Phys. Rev. Lett.* **1990**, *64*, 2953.
(13) De Kepper, P.; Castets, V.; Dulos, E.; Boissonade, J. *Physica D* **1991**, *49*, 161.
(14) Ouyang, Q.; Swinney, H. L. *Nature* **1991**, *352*, 610. Ouyang, Q.; Swinney, H. L. *Chaos* **1991**, *1*, 411.
(15) The abbreviation "CIMA" was proposed by P. De Kepper in 1990 and has been used extensively in private letters since then. In printed form it surfaced in 1991 in a paper by Winfree: Winfree, A. *Nature* **1991**, *352*, 568.
(16) Noszticzius, Z.; Horsthemke, W.; McCormick, W. D.; Swinney, H. L.; Tam, W. Y. *Nature* **1987**, *329*, 619.
(17) Tam, W. Y.; Horsthemke, W.; Noszticzius, Z.; Swinney, H. L. *J. Chem. Phys.* **1988**, *88*, 3395.
(18) Kshirsagar, G.; Noszticzius, Z.; McCormick, W. D.; Swinney, H. L. *Physica D* **1991**, *49*, 5.

0002-7863/92/1514-4290$03.00/0